

## The Effects of Ceramic Fillers on PMMA-Based Polymer Electrolyte Salted With Lithium Triflate, $\text{LiCF}_3\text{SO}_3$

K. W. Chew\* and K. W. Tan

Faculty of Engineering and Science, University Tunku Abdul Rahman, Jalan Genting Kelang, 53300 Setapak, Kuala Lumpur, Malaysia.

\*E-mail: [chewkw@utar.edu.my](mailto:chewkw@utar.edu.my)

Received: 21 September 2011 / Accepted: 11 October 2011 / Published: 1 November 2011

---

A series of poly(methyl methacrylate) PMMA based solid polymer electrolytes have been prepared and investigated by using a solution cast technique. The ethylene carbonate (EC) is chosen as a plasticizer,  $\text{SiO}_2$  and  $\text{Al}_2\text{O}_3$  were implemented as ceramic filler and the lithium triflate salt ( $\text{LiCF}_3\text{SO}_3$ ) as a main ions carrier to the polymer host systems. The conductivity behaviours of the samples prepared were studied by ac impedance spectroscopy (EIS), infrared spectroscopy (FTIR) and electron microscope technique (SEM). From the results obtained, it is proven that 25wt% of  $\text{LiCF}_3\text{SO}_3$  added into the PMMA–EC system shows best performance with the highest conductivity value of  $1.36 \times 10^{-5} \text{ Scm}^{-1}$ . The conductivity is further enhanced to  $2.05 \times 10^{-4} \text{ Scm}^{-1}$  with the addition of 5wt% of  $\text{Al}_2\text{O}_3$  and  $2.15 \times 10^{-5} \text{ Scm}^{-1}$  with addition 10wt% of  $\text{SiO}_2$ . The studies showed that the salt is helped to increase the number of charge carrier and provided free ions for conduction whereas ceramics fillers are capable of providing an extra conduction channels that further enhanced the conduction factor of the polymer electrolyte. Ionic conductivity increased with respect to the enhancement of the charge carried and filler, however excessive amount of these additives caused the conductivity to decrease. The results are further proven and supported by FTIR and SEM studies.

---

**Keywords:** PMMA, polymer electrolyte, impedance, FTIR, lithium triflate

### 1. INTRODUCTION

Thanks to today advanced science and technology development, many types of renewable or green energy sources such as wind, water and solar energy have been developed. However, due to the rapid increment of mobile devices usage, from a light mp3 player, mobile devices until the heavy duty electric vehicle power pack. The usage of those power sources are very frequent and repeatedly. Hence, the development of secondary rechargeable battery is considerably more important as compared to primary batteries. It's desirable to manufacture a smaller sized, high capacity and

lightweight battery which is environmental friendly and renewable. In this paper, the attention has been focused on the polymer electrolyte due to its high ionic conductivity as well as good mechanical properties [1, 2]. The presence of the solid polymer electrolytes eliminates the leakage and flammable problems as compare to liquid electrolytes. However, low conductivity of Solid polymer electrolyte (SPE) and mechanical integrity of gelled polymer electrolyte (GPE) have been a driving force for researchers to contribute more man power on the composite solid polymer electrolyte (CSPE) which allowing to fabricate a thin, flexible and various sized of battery. A number of methods have been reported to improve the ionic conductivity and mechanical stability of polymer electrolytes including the addition of plasticizer such as ethylene carbonate (EC) to form plasticized polymer matrix [3-6]. The addition of plasticizers also helps to reduce the glass transition temperature,  $T_g$  [7-8] that enhanced the ionic conductivity by increasing the segmental motion of the polymer.

The dielectric constant of the plasticizer is an important parameter that affects the ionic conduction. Higher dielectric constant results better dissociation of the salt as the number of free mobile charge carriers increased. In addition, adding an appropriate amount of lithium salt into the polymer matrix is significantly enhanced the ionic conductivity of the polymer electrolyte by increasing the number of charge carrier which provides free ions for conduction. The nano-sized filler particles such as  $\text{SiO}_2$  and  $\text{Al}_2\text{O}_3$  that intergraded into the solid polymer electrolyte increase the mechanical strength and enhanced the ionic conductivity [9-10]. It is believed that the ionic conductivity enhancement is due to its lewis acid-type interactions of mobile ionic species with the  $\text{O}^{2-}/\text{OH}^-$  groups on the surface of the filler grains which provide appropriate moving path for ions transportation between anode and cathode. The increase in conductivity also attributed to the decrease in the level of crystallinity in polymers due to the presence of fillers.

## 2. EXPERIMENTAL

### 2.1. Sample preparation

A series of Solid polymer electrolyte samples were prepared using solution cast technique. Poly(methyl methacrylate) PMMA with molecular weight of 996,000 was used as a host polymer. Whereby tetrahydrofuran (THF) is use as solvent to dissolve all mixtures of the solid electrolyte system. The mixture of host polymer, plasticizer, lithium salt, nano-sized filler and solvent were stirred up to several hours in order to obtain a homogeneous solution. The solution was then poured into the petri dishes and was left drying by solvent evaporation at ambient temperature until the films were formed. The films were then transferred into a desiccator for continuous drying before the test is carried out.

In this work, five types of polymer electrolyte systems were prepared. The first system consists of pure PMMA system which acts as reference. The second system is a PMMA system plasticized with controlled amount of EC that helps to soften the polymer matrix and the films formed are more flexible. The plasticized film is expected to have improved ionic conductivity even no lithium salts have being added into the system [11]. In the third system, appropriate amount of lithium salts

(LiCF<sub>3</sub>SO<sub>3</sub>) have been added into the predetermined composition from second system. The amount of host polymer is fixed but the amount of lithium salt is varies accordingly so that any changes of the conductivity values are mainly due to the addition of lithium salt. Finally, the fourth and fifth systems, Al<sub>2</sub>O<sub>3</sub> and SiO<sub>2</sub> are incorporated into the previous system that exhibits highest conductivity value with good mechanical strength.

2.2. Electrochemical Impedance spectroscopy (EIS)

In order to measure the impedance of the films of solid polymer electrolyte, the samples were cut into a round shape of 1 cm<sup>2</sup> and fit into the size of electrodes. The samples were then sandwich between two stainless steel plates for conductivity studies. The conductivity studies were carried out using ac impedance spectroscopy series Hioki 3531 with the operating frequency ranging from 50 Hz to 1 MHz. The measurement of bulk resistance (R<sub>b</sub>) can be determined from Cole-Cole plot as shown in Fig. 1. Thus the conductivity (σ) can be calculated using;

$$\sigma = \frac{t}{R_b A} \tag{1}$$

where *t* is the thickness of the sample (cm), *A* is the contact area of the electrode respect to electrolyte (cm<sup>2</sup>) and *R<sub>b</sub>* is the bulk resistance (Ω).

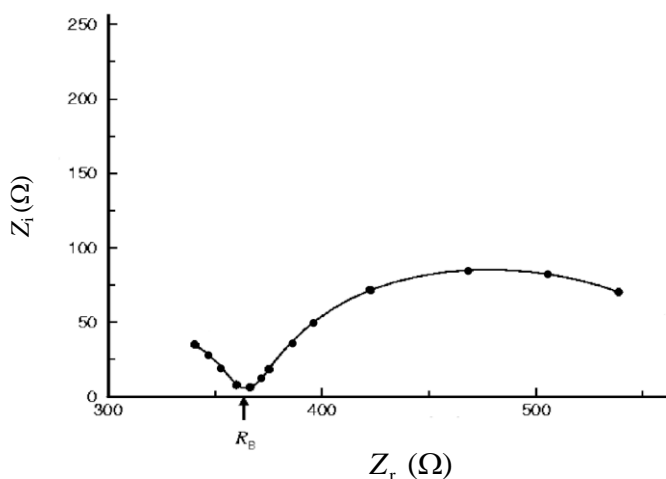


Figure 1. Cole-Cole plot of ac impedance spectroscopy

2.3. Fourier Transform Infrared Spectroscopy (FTIR)

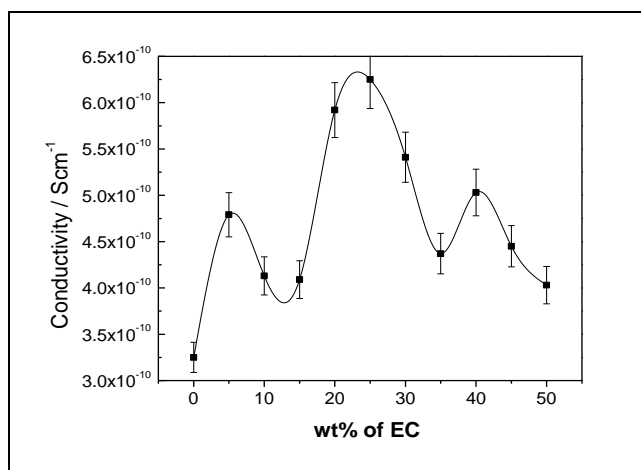
The test is carried out by Magna-IR 550 Spectroscopy Series II in the range of 400-4000 cm<sup>-1</sup> in order to identify the existence of ion-ion pairs and confirm the occurrence of complexation in the samples.

2.4. Scanning Electron Microscope (SEM)

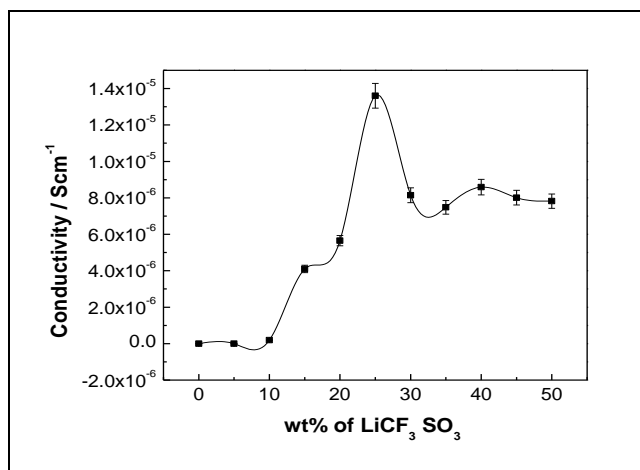
The microstructure imaging is carried out using high power scanning electron microscopy (SEM). The electron beam energy from few hundred eV to 50 keV is focuses into a thin beam of focal spot ranging from 1 nm to 5 nm. The exchange of energy between the electrons and the sample cause emission of secondary electron and electromagnetic radiation that can be detected and generate SEM images. The SEM has a large depth of field, and is capable of producing high resolution images, which means that closely spaced features can be examined at a high magnification.

3. RESULT AND DISCUSSION

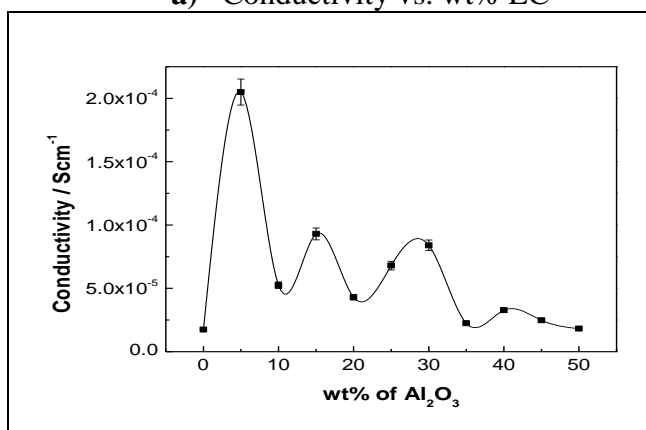
3.1. Ionic Conductivity



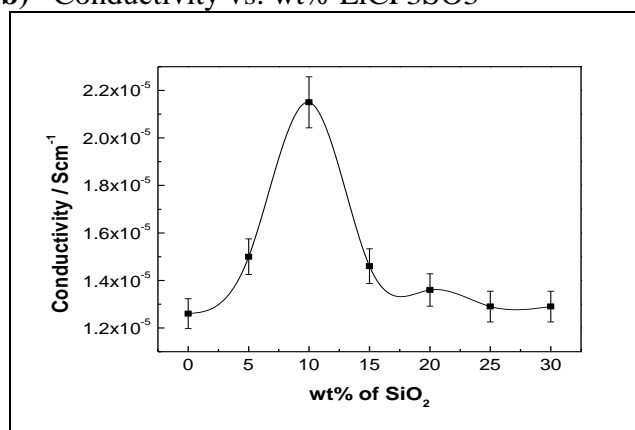
a) Conductivity vs. wt% EC



b) Conductivity vs. wt% LiCF<sub>3</sub>SO<sub>3</sub>



c) Conductivity vs. wt% Al<sub>2</sub>O<sub>3</sub>



d) Conductivity vs. wt% SiO<sub>2</sub>

Figure 2. a) Conductivity vs wt% EC b) Conductivity vs wt% LiCF<sub>3</sub>SO<sub>3</sub> c) Conductivity vs wt% Al<sub>2</sub>O<sub>3</sub> d) Conductivity vs wt% SiO<sub>2</sub>

From the *Rb* identified by Cole-Cole plot, the ionic conductivity is then be determined from equation (1).

Fig. 2 a) gives an rough idea on the crystallinity behaviour of PMMA, addition of EC plasticizer helps to increase the free volume and soften the polymer matrix of the polymer electrolyte thus rotation of polymer chain can occur more readily and the ion transport in the polymer electrolyte is faster as described by Rajendran et al. [12]. The PMMA itself may contains very small amount of minority carrier where addition of EC helps to lower the energy band of the ionic carrier. The maximum conductivity is achieved by addition of 25 wt% plasticizer (EC) which is  $6.25 \times 10^{-10} \text{ S cm}^{-1}$ . Relatively, the ionic conductivity for this system is low because no lithium salt is being doped into the system as a majority carrier.

With the addition of lithium salt ( $\text{LiCF}_3\text{SO}_3$ ) as shown in Fig. 2 b), the ionic conductivity of the polymer film is increased dramatically. The maximum conductivity is achieved at the addition of 25 wt% of  $\text{LiCF}_3\text{SO}_3$  gave the conductivity value of  $1.36 \times 10^{-5} \text{ S cm}^{-1}$ . Further increase of  $\text{LiCF}_3\text{SO}_3$  causes the conductivity to decrease due to the higher salt concentration, the conductivity decrease may be due to the increasing influence of the ion pairs, ion triplets, and higher ion aggregations, which reduces the overall mobility and degree of freedom. In net, the number of effective charge carriers that transit between anode and cathode are relatively reduced, MacCallum et al. [13].

In the Fig. 2 c), with additional of 5 wt%, of  $\text{Al}_2\text{O}_3$  filler the best ionic conductivity is achieved at  $2.05 \times 10^{-4} \text{ S cm}^{-1}$ . Referring to the study of Croce et al. [14], Lewis acid-base type oxygen and OH surface groups on alumina grains interact with the cations and anions and therefore providing additional sites creating favourable high conducting pathway in the vicinity of grains for the migration of ions. Dissanayake et al. [14] reported that further addition of the filler grain after its saturated state, the conductivity decreased by blocking effect imposed by the more abundant alumina grains, the long polymer chains is “immobilized” and causes the conductivity to decrease.

Same results is observed for Fig. 2 d), with additional of 10 wt% of  $\text{SiO}_2$  the ionic conductivity increased to  $2.15 \times 10^{-5} \text{ S cm}^{-1}$  result by Lewis acid-base reaction between the  $\text{SiO}_2$  filler surface group with the polymer chain attributed to the enhancement of the ionic conductivity. Scrosati et al. [15] claims that the increment of the ionic conductivity with the addition of  $\text{SiO}_2$  is due to an increase in free ion concentration. Hyung-Sun Kim et al. [19] reported that  $\text{SiO}_2$  reduces the glass transition temperature and crystallinity of the polymer, and allows the amorphous polymer to provide specific liquid-like characteristics. In addition, the addition of filler to a polymer matrix is found to improve the ionic conductivity by reducing the crystallization tendency. Further addition of  $\text{SiO}_2$  causing the ionic conductivity to decrease due to the blocking effect similarly to the effect in  $\text{Al}_2\text{O}_3$  where the grains are get close to one another, leading to the decreasing of the conductivity.

### 3.2. Temperature Dependence of Polymer Electrolytes

Solid polymer electrolytes with best ionic conductivity at room temperature will be selected for further verification of their Arrhenius behaviour. Impedance measurement for temperature ranging

from 300 K to 413 K is carried out. From Fig. 3, it is clearly observed that the polymer electrolytes showed the Arrhenius behaviour. Jeon et al. [16] revealed that the ionic conductivity enhanced almost linearly with respect to the increment of temperature although there were slight curvature in the plots. They also explained that as the temperature increase, the degree of freedom of polymer electrolyte increases and thus produced free volume. As a result, ions, solvated molecules or the polymer segment can move into the free volume easily and lead to enhancement of the ionic conductivity.

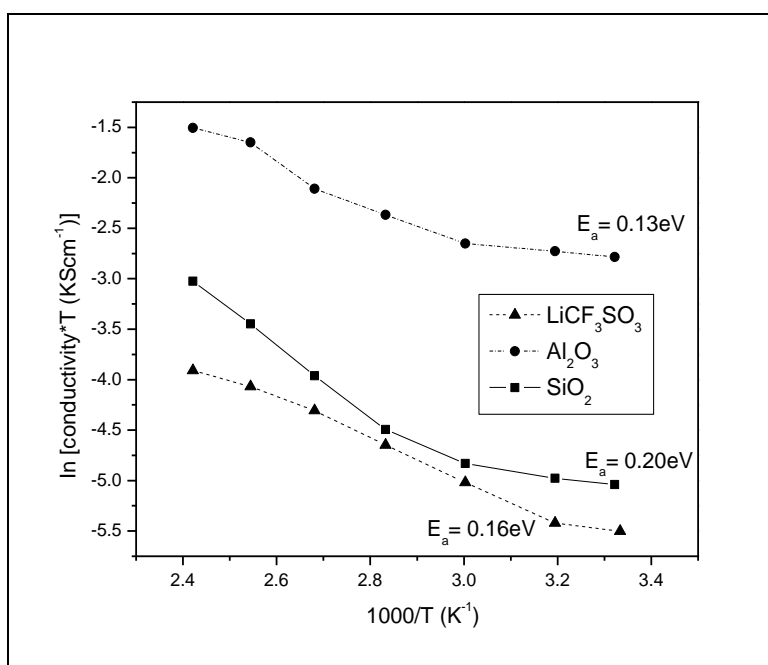


**Figure 3.** Temperature dependence of polymer electrolyte with the best ionic conductivity in each polymer system

As shown in the Fig. 3, Activation energy ( $E_a$ ) for samples added with 25 wt% LiCF<sub>3</sub>SO<sub>3</sub> lithium salt, 5 wt% of Al<sub>2</sub>O<sub>3</sub> filler and 10 wt% of SiO<sub>2</sub> filler at different test temperatures are 0.16 eV, 0.13 eV and 0.20 eV. Ramesh et al. [17] claimed that the low  $E_a$  is due to the amorphous nature of the polymer electrolytes that facilitate the fast Li<sup>+</sup> ion motion in the polymer network. It can be seen that 5 wt% of Al<sub>2</sub>O<sub>3</sub> filler added samples has the higher ionic conductivity and lower  $E_a$  compared with the other samples.

### 3.3. FTIR Studies

In this work, FTIR spectra of various compositions of PMMA-based polymer electrolyte were carried out. Based on the observation shown in Fig. 4, It can be seen that C-O stretching at 1290 cm<sup>-1</sup>, O-CH<sub>3</sub> deformation band at 1387 cm<sup>-1</sup>, C=O stretching band at 1733 cm<sup>-1</sup>, CH<sub>3</sub> bending band at 1441 cm<sup>-1</sup> and CH<sub>3</sub> asymmetric stretching band at 2953 cm<sup>-1</sup>. C-O-C bending which appear at 841 cm<sup>-1</sup> is shifted to 844 cm<sup>-1</sup> caused by the additional of the EC into the system. Due to the effect of the EC

plasticizer, the absorption peak at  $1811\text{ cm}^{-1}$  of pure PMMA was shifted to  $1857\text{ cm}^{-1}$  for the C=O stretching.

With the addition of LiCF<sub>3</sub>SO<sub>3</sub> into the system, the absorption peak at the  $1055\text{ cm}^{-1}$  shifted to  $1033\text{ cm}^{-1}$  in all the polymer electrolyte due to the existence of the vibration mode symmetric SO<sub>3</sub> of the LiCF<sub>3</sub>SO<sub>3</sub>. The deformation of CF<sub>3</sub> caused the absorption peak at  $764\text{ cm}^{-1}$  shift to  $774\text{ cm}^{-1}$  due to the additional 25 wt% of LiCF<sub>3</sub>SO<sub>3</sub>.

The vibration modes of Al=O, H<sub>2</sub>O rocking vibrations and O-H stretching of the Al<sub>2</sub>O<sub>3</sub> were found at  $1384\text{ cm}^{-1}$ ,  $1634\text{ cm}^{-1}$ , and  $3500\text{ cm}^{-1}$ . Song et al.[18] Revealed that the appearance of O-H stretching vibration indicates the presence of the oxygen-hydrogen (O-H) groups at the surface of Al<sub>2</sub>O<sub>3</sub>, and thus Lewis acid-base type oxygen and OH surface groups on the alumina grains to interact with the ions of the lithium salt.

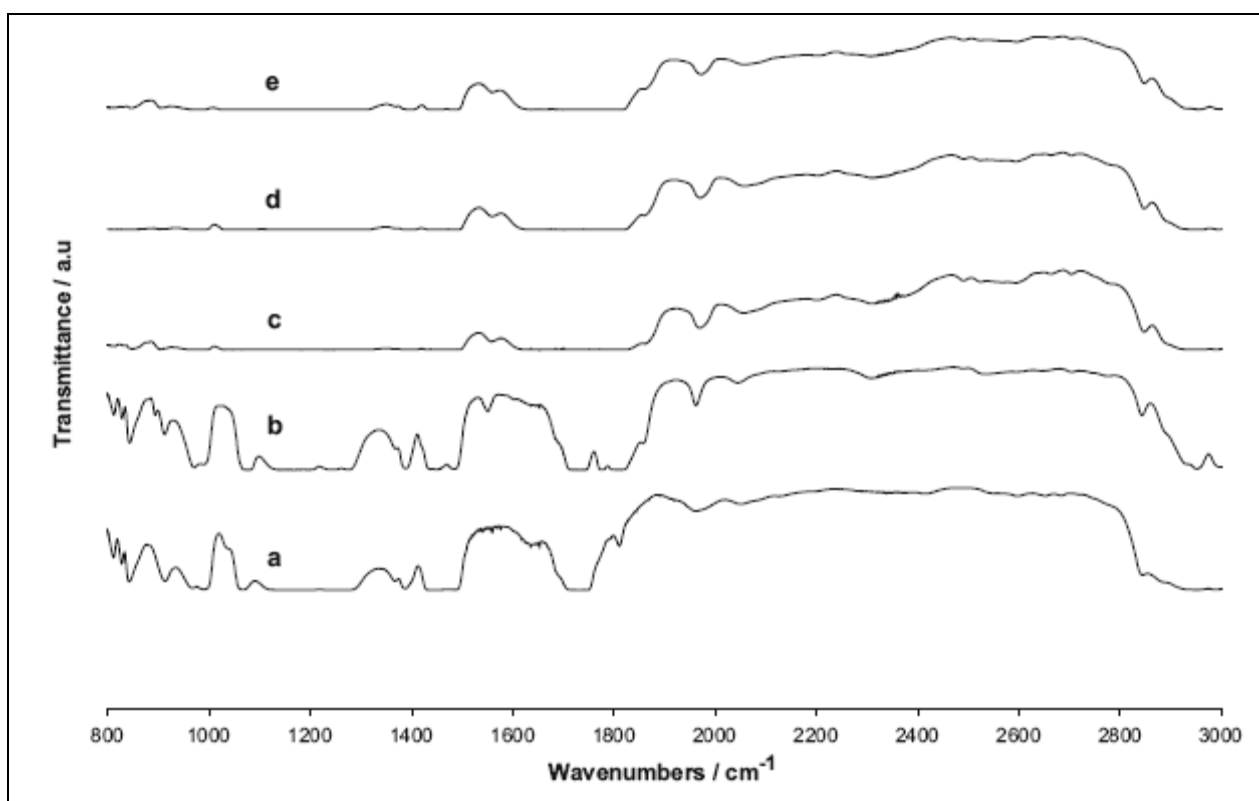
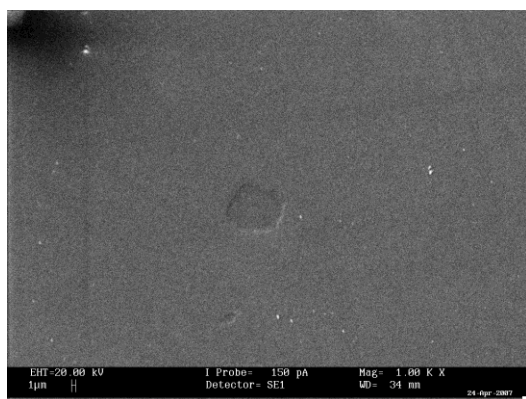


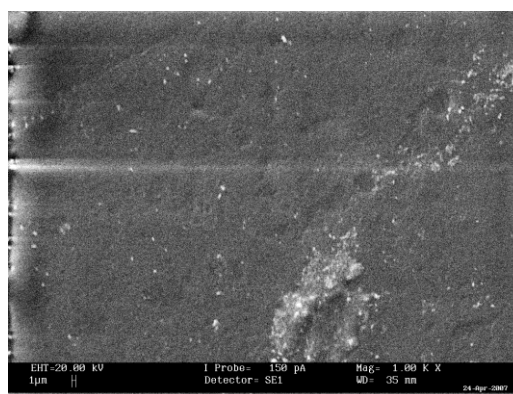
**Figure 4.** The FTIR spectra of a) pure PMMA b) 25 wt% EC c) 25 wt% LiCF<sub>3</sub>SO<sub>3</sub> d) 5 wt%, of Al<sub>2</sub>O<sub>3</sub> e) 10 wt% of SiO<sub>2</sub>

The O-H bending modes of hydrogen-bonded and isolated silanolic groups were determined at wave number  $813\text{ cm}^{-1}$  and  $971\text{ cm}^{-1}$  respectively. The absorption peak at  $1106\text{ cm}^{-1}$  indicated the existence of Si-O stretching in the SiO<sub>2</sub> filler. The O-H deformation vibration of the surface hydroxyl group of fumed silica was found at  $1635\text{ cm}^{-1}$ , indicating the existence of OH surface groups for the Lewis acid-base interaction.

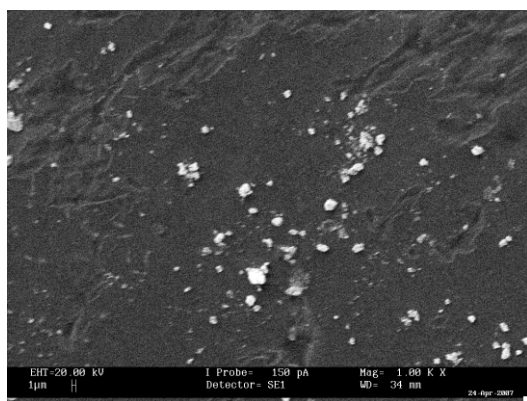
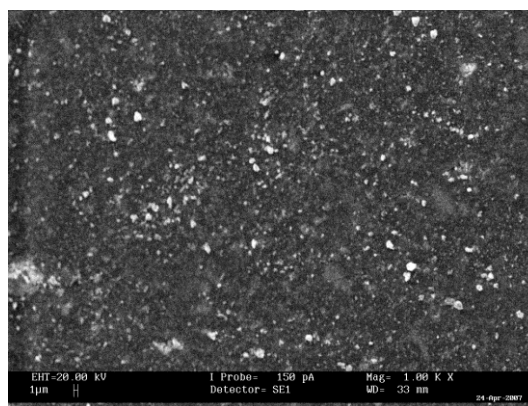
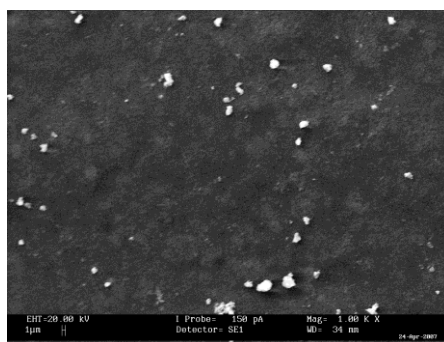
## 3.4. Scanning Electron Microscopic (SEM)



a) SEM of pure PMMA



b) SEM of PMMA (75): EC (25)

c) SEM of PMMA/EC(75):LiCF<sub>3</sub>SO<sub>3</sub>(25)d) SEM of PMMA/EC/LiCF<sub>3</sub>SO<sub>3</sub>(95):Al<sub>2</sub>O<sub>3</sub>(5)e) SEM of PMMA/EC/LiCF<sub>3</sub>SO<sub>3</sub>(90):SiO<sub>2</sub>(10)

**Figure 5.** a) SEM of pure PMMA b) SEM of PMMA(75):EC(25) c) SEM of PMMA/EC(75):LiCF<sub>3</sub>SO<sub>3</sub>(25) d) SEM of PMMA/EC/LiCF<sub>3</sub>SO<sub>3</sub>(95):Al<sub>2</sub>O<sub>3</sub>(5) e) SEM of PMMA/EC/LiCF<sub>3</sub>SO<sub>3</sub>(90):SiO<sub>2</sub>(10)

Fig 5 shows microstructures of solid polymer thin films obtained from different chemical mixtures. Pure PMMA sample as shown in Fig. 5 a) has a smooth surface with not much pores exist. It can be observed that the spherical pore size of PMMA is around 15.1  $\mu\text{m}$ . When EC was added into PMMA (Fig. 5 b)), a complexation with a rougher surface is produced with more pores. These rough surfaces provide better surface exposure thus help to slightly increase the ionic conductivity as



compare to pure PMMA. This observation result is agreed with the conductivity studies that shows slight increment in conductivity value when EC was added into the pure PMMA sample. In Fig. 5 c), the spherulite form surface was observed when doped with  $\text{LiCF}_3\text{SO}_3$  which indication the interaction between host polymer PMMA and plasticizer EC and changed the system to amorphous nature. As shown in Fig. 5 d). The morphology of polymer electrolyte is totally altered upon addition of filler. Dispersion of the  $\text{Al}_2\text{O}_3$  filler into the previous optimum systems, the nano-sized  $\text{Al}_2\text{O}_3$  interacted with free ions where the alumina grains were found smaller in size and even disperse across the surface. This effect attributes to the highest ionic conductivity due to the more ion path way which cause better ion mobility and ion aggregates dissociation that provide more charge carrier in composite solid polymer electrolyte. Fig. 5 e) shows the polymer sample with the dispersion of  $\text{SiO}_2$ , it can be seen that the sample tends to dissolve more lithium salt and ion aggregates and provide amorphous region in polymer electrolyte. The dispersion of  $\text{SiO}_2$  nano-particles reveals the aggregations among the nano-sized particle via hydrogen bonding on the surface of silica atoms. Due to the formation of three-dimensional network as a result of the hydrogen bonding among aggregates. So, large volumes of filler are being entrapped, it accounts for the highest ionic conductivity by enhancing the ionic migration among the polymer matrix. Although  $\text{SiO}_2$  is not giving highest ionic conductivity in overall polymer electrolyte, but it is still providing better ionic conductivity compare to filler-free polymer electrolyte system.

#### 4. CONCLUSION

PMMA-based polymer electrolytes were prepared by solvent casting technique. The polymer electrolytes added with  $\text{LiCF}_3\text{SO}_3$  lithium salt and adopted by  $\text{Al}_2\text{O}_3$  and  $\text{SiO}_2$  filler has been confirmed from EIS, FTIR and also SEM studies. With the additional of 25 wt% of  $\text{LiCF}_3\text{SO}_3$  into plasticized PMMA, ionic conductivity of  $1.36 \times 10^{-5} \text{ S cm}^{-1}$  has been achieved. In order to bring the ionic conductivity to higher level, adding nano-sized filler is necessary. By additional either 5 wt% of  $\text{Al}_2\text{O}_3$  or 10 wt% of  $\text{SiO}_2$  to the system, the value of ionic conductivity obtained is  $2.05 \times 10^{-4} \text{ S cm}^{-1}$  or  $2.15 \times 10^{-5} \text{ S cm}^{-1}$  respectively. At the same time, the mechanical properties of the particular composite solid polymer electrolyte are enhanced accordingly to the filler dispersed into the polymer electrolytes. The ionic conductivity of polymer electrolytes also has been measured in between 300 K to 413 K. It is proved that the variation of temperature affected to the ionic conductivity such as increasing the temperature, the ionic conductivity increased. Hence Arrhenius behavior was determined.

The infrared spectroscopy indicated that complexation has occurred between polymer and plasticizer, and also between polymer, plasticizer and salt. The occurrence of the complexation was determined through the shift of peaks, change in peak intensity and appearance of new peak in the FTIR spectrum. The effect of interaction between host polymer, plasticizer, lithium salt and filler is obtained through SEM characterization.

## References

1. N. S. Choi, Y. G. Lee, J. K. Park, J. M. Ko, *Electrochim Acta*, 46 (2001) 1581.
2. A.M. Stephen, R. Trirunakaran, N. G. Renganathan, V. Sundaram, S. Pituchumani, N. Muniyandi, R. Gangadharan , P. Ramamoorthy, *J. Power Sources*, 81-82 (1999) 752.
3. G. Nagasubramanian, A. I. Attia, G. Halpert, *J. Appl Electro Chem*, 24 (1994) 298.
4. P. E. Tallworth, S. G. Greenbaum, F. Croce, S. Slane, M. Salomon, *Electrochim Acta*, 40 (1995) 2137.
5. E. Morales, J. L. Acosta, *Solid State Ionics*, 96 (1997) 99.
6. S. Abbrent, J. Lindgren, J. Tegenfeldt, A. Wendsjo, *Electrochim Acta*, 43 (1998) 1185.
7. M. Kakihana, S. Schantz, L. M. Torell, *J. Chem Phys*, 92 (1990) 6271.
8. A. Bernson, J. Lindgren, *Solid State Ionics*, 60 (1993) 37.
9. Y. Tominaga, S. Asai, M. Sumita, S. Panero, B. Scrosati, *J. Power Sources*, 146(2005) 402.
10. Y. Liu, J. Y. Lee, L. Hong, *J. power sources* 109 (2002) 507.
11. W. Lishi, H. Yudai and J. Dianzeng, *Solid State Ionics* 177 (2006) 1477.
12. S. Rajendran, O. Mahendran and R. Kannan, *J. Physics and Chemistry of Solids* 63 (2002) 303.
13. J. R. MacCallum , A. S. Tomlin, and C. A. Vincent, *European Polymer J.*, 22 (1986) 787.
14. M. A. K. L. Dissanayake, P. A. R. D. Jayathilaka, R. S. P. Bokalawala, I. Albinsson, and B. E. Mellander, *J. Power Sources*, 119 (2003) 409.
15. B. Scrosati, F. Croce and L. Persi, *J. Electrochemical Soc*, 147 (2000) 1718.
16. J. D. Jeon, S. Y. Kwak, and B. W. Cho, *J. Electrochemical Soc.*, 152 (2005) 1583.
17. S. Ramesh and A. K. Arof, *Mat. Scn. & Eng. B-solid state Mat. for Advanced Technology*, 85 (2001) 11.
18. H. J. Song, Z. Z. Zhang, and X. H. Men, *Surface & Coating Tech*, 206 (2006) 3767.
19. S. K. Hyung, S. K. Kyong, C. Won-II, W. C. Byung, W. R. Hee, *J. Power Sources*, 124 (2003) 221.